JOURNAL OF MATERIALS SCIENCE 31 (1996) 5933–5940

Mechanical and structural characterization of Nicalon fibre-reinforced borosilicate glass

S. M. BLEAY*, B. HARRIS, V. D. SCOTT, R. G. COOKE, F. A. HABIB
School of Materials Science, University of Bath, Bath BA2 7AY, UK

Work carried out on Nicalon/glass composites as part of a larger programme on the structure and properties of ceramic-matrix composites is described and is in contrast to publications by this group on related materials in which the interfacial bonding was quite different. As a consequence of differences in manufacturing, the interfacial bonding in these more recent materials is substantially improved, as demonstrated by the markedly improved level of shear stiffness (by a factor of 2–3) and the higher level of interlaminar shear strength (some 50%–100% improvement). There is, however, an accompanying deterioration in the tensile and flexural strengths. The fracture mode of these Nicalon/borosilicate-glass composites is strongly influenced by the cristobalite content and the properties of the interface, both of which are controlled to a large extent by the manufacturing parameters.

1. Introduction

As part of a wider programme on ceramic-matrix composites, the characteristics of a range of composites consisting of borosilicate glass reinforced with Nicalon silicon carbide fibre have been studied, and several papers dealing with the structure and mechanical properties of these materials have already been published [1–4]. Although, from a practical point of view, the qualities of this material are less well adapted for application at high temperature, in air-breathing gas turbines, for example, than those of their more robust counterparts with glass-ceramic matrices, they do possess a number of virtues when compared to those materials, especially for experimental investigations of ceramic-matrix composites (CMCs) in general, the most obvious being the lower processing temperature which results in fewer problems relating to thermal stress and chemical compatibility. The value of such an experimental material has been well recognized, as witness the extensive studies carried out on Nicalon/borosilicate composites as part of the USA/Japan NEDO programme [5].

In the course of a programme in which one component of the research relates to optimization of the manufacturing conditions for specific applications, there will be an obvious need to evaluate the processing/structure/properties inter-relationship. The materials for this study were supplied by another contributor to the programme, however, and it was not possible, for practical and commercial reasons, for each stage of the manufacturing programme to be matched by an equally intensive survey of structure and properties. Thus, having already reported extensively on material manufactured early in the programme, we subsequently had access to further batches of material for which different processing conditions had modified the fibre/matrix bond. This paper deals with this later batch of material and makes comparisons with the conclusions from our earlier work.

2. Experimental procedure

2.1. Composite plates

The materials used in this work were provided by Rolls Royce. For commercial reasons, no details of manufacturing conditions can be given, but it is assumed that the procedures used were broadly similar to those described by Sambell *et al.* [6] and Dawson *et al.* [7]. The numbering system used for some of the composite plates referred to here relates to the manufacturing/supply protocols, but is retained here for convenience.

In all, some 16 plates of hot-pressed SiC/borosilicate composite material were provided for this work. These were of various lay-ups, including $(0)_{12}$ (unidirectional), $(0, 90)_{3s}$ and $(\pm 45, 0_2)_s$. The plates were from a range of different batches prepared by the manufacturer, and their quality was variable. The composites were supplied in the form of plates, hot-pressed to dimensions of 100 mm × 100 mm by approximately 2 mm. Microscopic examination of the as-manufactured materials revealed no matrix microcracking in the composites following manufacture. The fibre volume fraction of the plates varied slightly, that of earlier samples being approximately 0.34, while in later samples the figure was between 0.37 and 0.44.

* *Present address*: Structures and Materials Centre, DRA, Farnborough, Hampshire, UK.

0022–2461

2.2. Nicalon fibres

A sample of Nicalon fibre was supplied from a bobbin in the as-sized condition by AEA technology, Harwell. Some fibres were retained in this condition, while the remainder had the PVA size burnt away in a gas flame. Bundles of sized and de-sized fibres were given a thin conductive coating of gold and mounted for examination by scanning electron microscopy. Compositional analysis of the surfaces of the fibres was performed by energy-dispersive X-ray spectrometry (EDS).

In order to assess fibre degradation during processing, a bundle of Nicalon fibres was etched out of a Nicalon/borosilicate composite by immersion in 5% HF for 4 h. A bundle of de-sized fibres was given the same immersion to ensure that any observed difference arose from the fibres themselves rather than as a result of the etching. Single-fibre tests were performed on batches of 30 fibres from each bundle according to ASTM D3379-75 [7] at a gauge length of 30 mm and crosshead speed of 0.5 mm min^{-1} in an Instron model 1122. Fibre diameters were measured for each fibre with a Watson image-splitting eyepiece on an optical microscope.

2.3. Mechanical testing

Tensile properties were measured on unwaisted test coupons of dimensions 20 mm × 100 mm, cut from the hot-pressed plates by means of a water-cooled diamond saw. Soft aluminium tabs were bonded with Araldite epoxy resin to the ends of each tensile specimen to prevent damage in the test machine grips. Tensile tests were carried out in an Instron machine at a crosshead speed of 0.5 mm min^{-1}. For extension measurements, a Wallace optical extensometer with 25 mm gauge length was used, and for more sensitive strain measurements for the determination of elastic moduli, pairs of strain gauges at 90° to one another were bonded on to one face of tensile specimens. Shear modulus measurements were obtained by the ultrasonic pulse velocity method.

Flexural tests were carried out in three-point bending on samples approximately 10 mm wide at span-to-depth ratios of 40 for unidirectional material and 25 for cross-plied composites, and the interlaminar shear strengths of the unidirectional materials were measured in short-beam shear tests on samples with a span-to-depth ratio of 10. The shear strengths of the more recent materials have also been determined by the Iosipescu method.

The tensile tests were monitored with acoustic emission analysis equipment. Acoustic emission (AE) signals the occurrence of localized damage, on both the microstructural and macroscopic scales, during loading, and the monitoring of these stress-wave events can provide information about the damage mechanisms in composites and other materials. The stress-wave signals were collected by a conventional PZT transducer (resonant frequency 150 Hz) and processed by a Marandy amplitude analysis system which stores the digital AE data as a function of time, together with A–D converted load and strain signals, on a computer. Results were analysed and graphed with the aid of conventional spread-sheet software. We have already made extensive reference to our use of these techniques for the study of failure processes in CMCs [1, 8, 9].

2.4. Microscopy

Samples were prepared for optical microscopy by cutting sections with a low-speed, water-cooled diamond saw and mounting in cold-curing epoxy resin. Polishing was carried out by planar grinding of the samples followed by finishing with diamond slurries on Buehler Metlap wheels of decreasing hardness to obtain the final finish.

Thin-foil specimens were prepared for transmission electron microscopy (TEM) by first drilling discs from bulk composite with a diamond-tipped coring drill, followed by mechanical grinding, dimpling and ion-beam thinning to produce an electron-transparent area for analysis. Compositional information was obtained by using an EDS system fitted to the TEM.

Powdered samples of each plate were examined by X-ray diffraction (XRD) to obtain a quantitative estimate of the degree of crystallinity in the glass matrix. This was carried out by the internal standard technique [10].

Values of interfacial friction stress were obtained from measurements on polished sections by the micro-indentation technique developed by Marshall and Evans [11].

3. Results

3.1. Structure and properties of Nicalon fibres

The PVA sizing applied to the Nicalon fibre is clearly visible in the scanning electron micrograph in Fig. 1a, and EDS confirmed that this layer consisted predominantly of carbon. After desizing the surface is smooth (Fig. 1b), and EDS studies indicate an oxygen-enriched surface.

Results of tensile tests on single fibres are shown in the Weibull plots of Fig. 2. The desized fibres gave a tensile strength of 1.67 ± 0.24 GPa, while the sample of fibres extracted from the composite (see Fig. 1c) gave a value of 1.60 ± 0.4 GPa. These are not significantly different, but despite the similarity in the mean values, it can be seen from Fig. 2 that there is a far greater degree of scatter in the data set for the extracted fibres. The values of Weibull shape parameter, m, are found from Fig. 2 to be 7.3 for de-sized and 3.9 for extracted fibres, respectively. It is perhaps to be expected that the variability of fibre strength would increase after the fibres have undergone the rigours of a high-temperature fabrication programme involving the possibility of fibre/matrix reaction, but it is difficult to see how this could occur without the fibre strength also being affected. We note, particularly, that the strength of even the unprocessed fibre is considerably lower than the strength values suggested by the manufacturer's literature, namely 2.5–3 GPa.

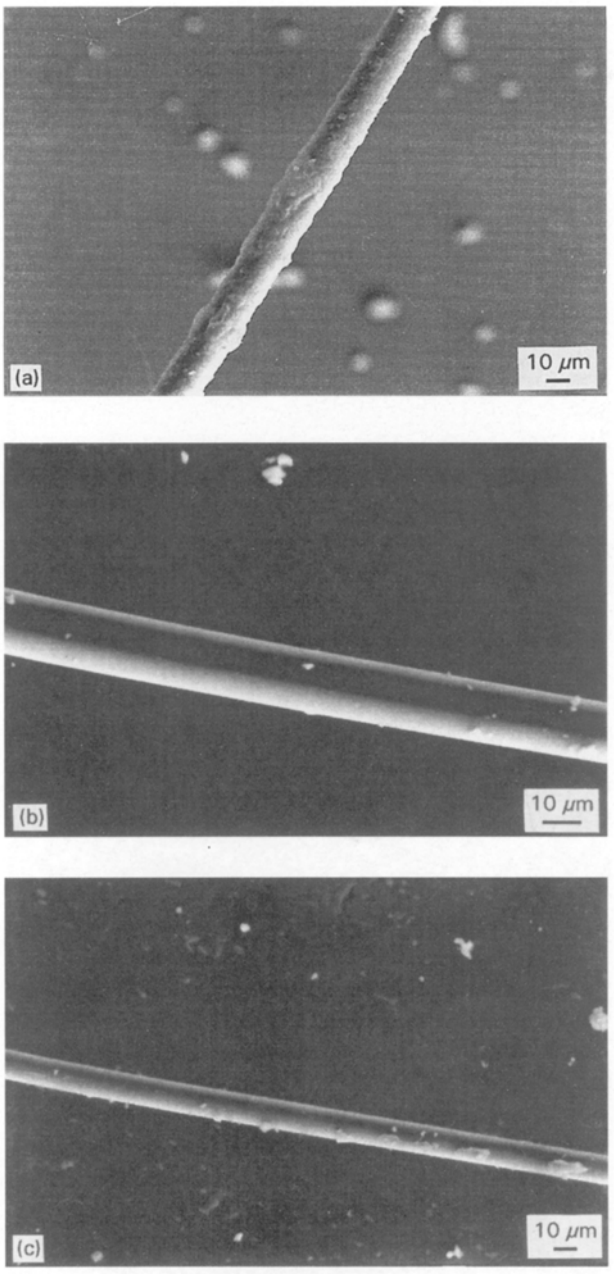

Figure 1 Scanning electron micrographs: (a) sized Nicalon fibre, (b) desized Nicalon fibre, (c) Nicalon fibre extracted from a borosilicate glass matrix.

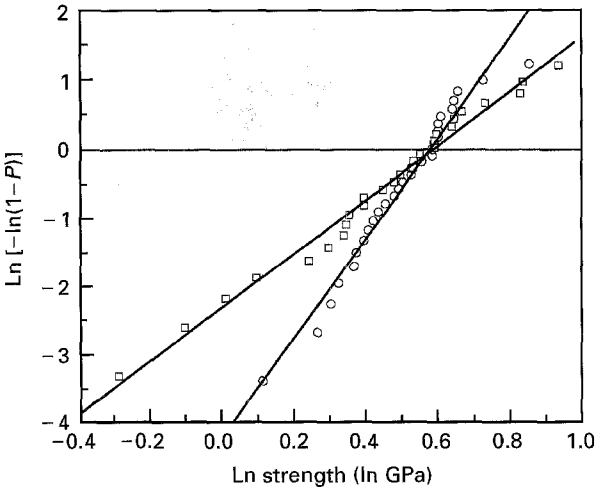

Figure 2 Weibull plots of strength measurements on Nicalon fibres in the (○) desized condition and (□) after extraction from a Nicalon/borosilicate composite. *m*: (○) 7.3, (□) 3.9.

3.2. Characteristics of composite plates

3.2.1. Structure

The R3(1) batch of composite was typical of material manufactured and tested in the earlier stages of this programme. It had a homogeneous fibre distribution and a fibre volume fraction of 0.33 (Fig. 3a). The matrix had a cristobalite content of 48 ± 3 vol %, microcracks being associated with the cristobalite particles. When the interface was imaged in the TEM, a light diffusion band about 200 nm thick was identified in the outer layers of the fibre, as shown in Fig. 3b. Sodium depletion was found in the glass adjacent to the fibre, and significant compositional differences were found in the interfacial zone. The interface contained silicon and oxygen, with large amounts of carbon and sodium. Small traces of potassium and calcium were also present, these elements constituting less than 0.2 wt%. The interfacial friction stress was the lowest of the samples examined, at 5 ± 1 MPa but, rather than showing pull-out, the matrix fragmented and fell away from the fibres before reaching peak load to leave long lengths of clean fibre with occasional "collars" of matrix, as in Fig. 3c. In the plates used for the bulk of the mechanical tests, it was apparent that there was a substantial amount of porosity, as shown in Fig. 3d and e (the latter also shows the usual signs of the presence of cristobalite).

Composite R71(2) was typical of the later batch of material provided for evaluation in this programme. It had a homogeneous fibre distribution, a fibre volume fraction of 0.44 but, by contrast with R3(1), it had a matrix cristobalite content of only 9 ± 3 vol %. Compositionally, the fibre/matrix interface resembled that of R3(1), but the diffusion band was only 50 nm in depth compared to 200 nm in R3(1). The fibre surface was more serrated and less carbon was present. Micro-indentation tests gave an interfacial friction stress value of 12 ± 2 MPa, and the fracture surface resembled that of the optimized Harwell material discussed in an earlier paper [8].

3.2.2. Mechanical properties

A summary of the mechanical properties of the SiC/borosilicate composites examined in this investigation is given in Table I. In view of the relatively small amounts of material available, no attempt is made here to give any indication of statistical parameters for these results. The table includes results for materials of both the early and later batches. Comparison of the results for the earlier six unidirectional plates (coded R1–R6) and the more recent pair (R71) shows the results of changing processing conditions between the two production periods. The mean fibre volume fractions of the newer plates are of the order of 0.4 instead of 0.34, but the tensile strengths of the newer plates are significantly lower (and also more variable: 300–600 MPa). The failure strains have also

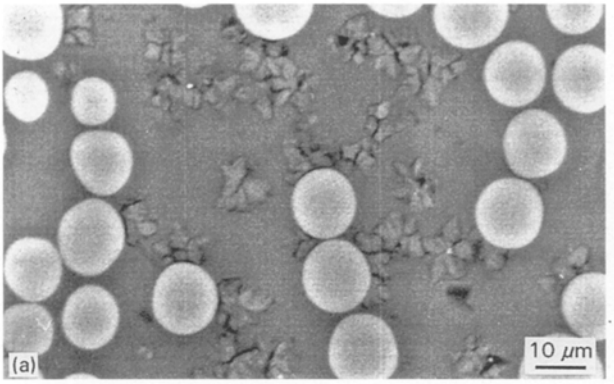

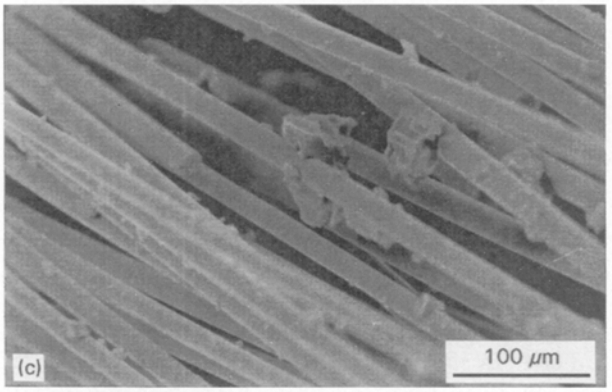

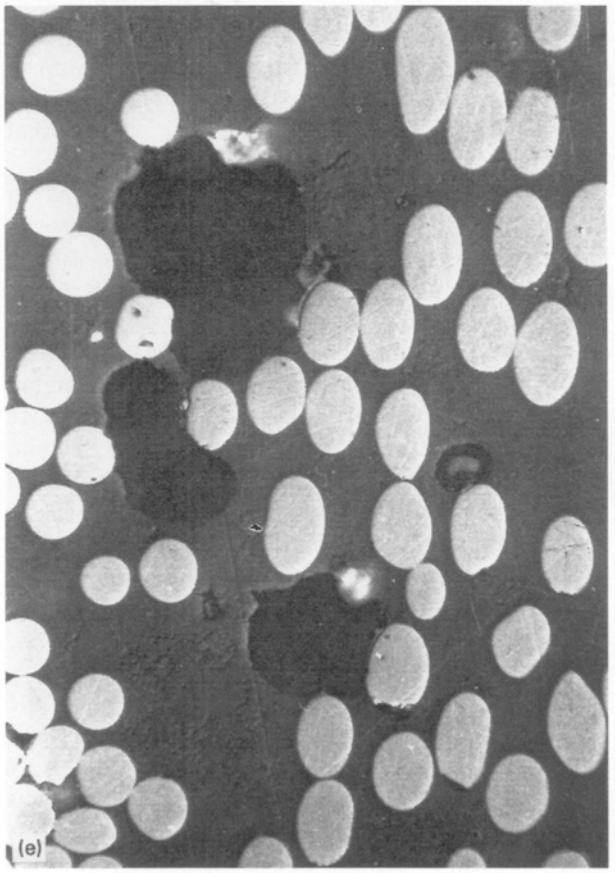

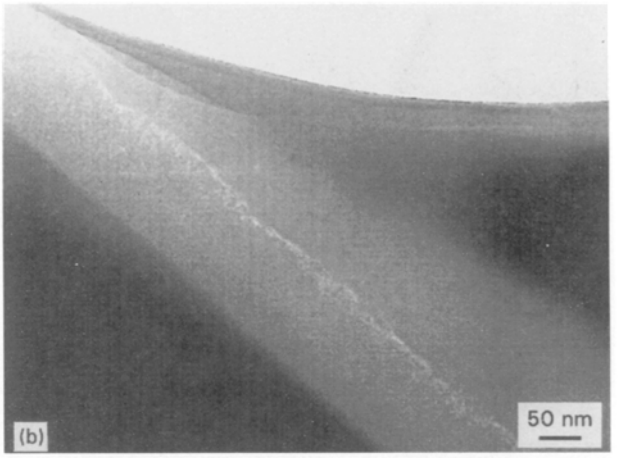

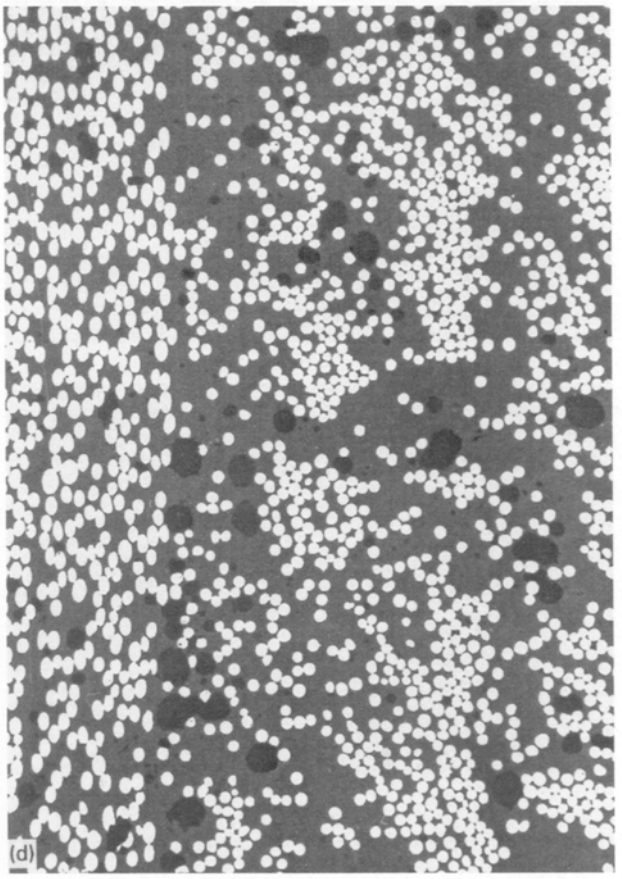

Figure 3 (a) Back-scattered electron image of composite R3(1). (b) Transmission electron micrograph of the fibre/matrix interface in composite R3(1). (c) Scanning electron micrograph of the fracture surface of composite R3(1). (d) Optical micrograph of porosity in composite R91, ×160. (e) Optical micrograph of porosity in composite R91, ×420.

fallen as a consequence of the changes in processing conditions.

It is interesting to note that while Young's modulus of the various unidirectional samples is apparently not very sensitive to the processing conditions, the shear modulus, determined from ultrasonic pulse velocities, show a marked improvement in the shear stiffness of the newer plates, by a factor of more than two. This improvement, which appears to reflect better bonding in the later materials, is also indicated by the improvement in the interlaminar shear strength. We noted earlier that the first batch of SiC/borosilicate materials received from the manufacturer contained a high cristobalite content, and it would have been natural to suppose that this partial crystallization could have adversely affected the mechanical properties of the composites. It seems clear, now, however, that this could not have been the case,

TABLE 1 Summary of mechanical properties of experimental Nicalon/borosilicate composites

Lay-up	density (g cm^{-3})	V_f	Tensile modulus (GPa)	Tensile strength (MPa)	Failure strain (%)	Poisson's ratio	Flexural modulus (GPa)	Flexural strength (MPa)	Shear modulus (GPa)	Shear strength (MPa)	ILSS (MPa)
First batch											
$ud(0)_{12}$	2.35	0.34	95	726	1.2	0.14	92	1280	14	–	28
$(0,90)_{3s}$	2.42	0.34	80	343	0.82	0.06	65	650	12	–	–
Second batch											
$ud(0)_{12}$	2.32	0.42	106	487	0.53	0.18	96	922	34	150	41
$(0,90)_{3s}$	2.10	0.40	87	89	0.24	0.15	56	325	31	57	–
$(\pm 45,0_2)_s$	2.29	0.36	90	253	0.8	0.26	55	379	34	149	–

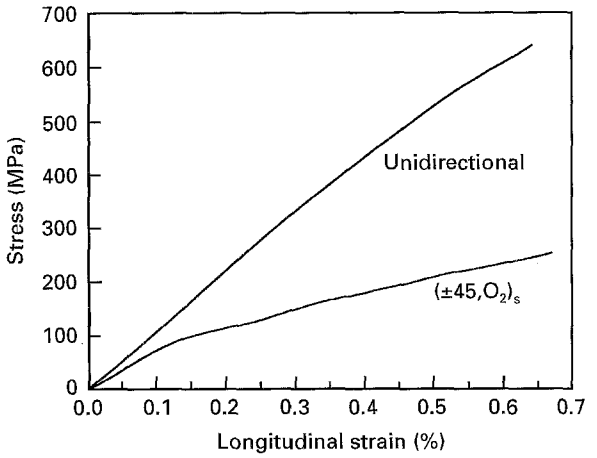

Figure 4 Stress–strain curves for unidirectional and $(\pm 45,0_2)_s$ Nicalon/borosilicate composites.

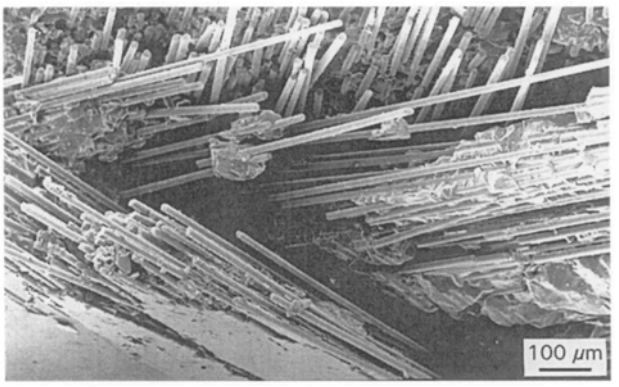

Figure 5 Fibre pull-out in the fracture surface of a $(\pm 45,0_2)_s$ Nicalon/borosilicate composite.

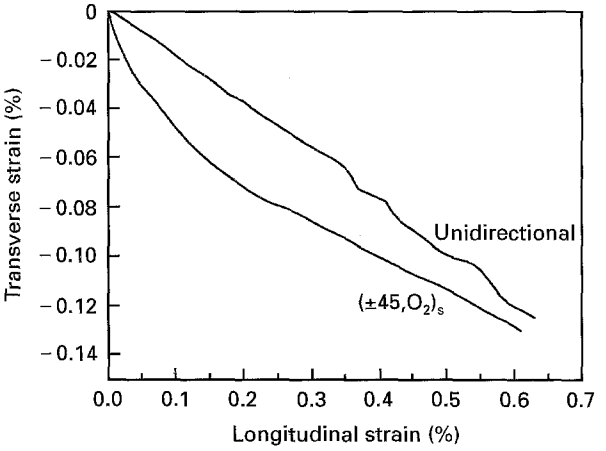

Figure 6 Transverse strain, ε_{22}, as a function of axial strain, ε_{11}, for unidirectional and $(\pm 45,0_2)_s$ Nicalon/borosilicate composites.

because the newer unidirectional plates, which contained less than 10 vol% cristobalite, are much weaker than the earlier materials. It must be said, however, that absolute values of strength may not tell the whole story, because failure of the early batch of material occurred in such a way as to render it useless as a structural material.

3.2.3. Stress–strain curves

Fig. 4 shows stress–strain curves for the later unidirectional composite (R71,2) and the $(\pm 45,0_2)_s$ material (R91,2). The curve for the unidirectional material is initially linear up to about 0.35% strain, and thereafter shows a gradually reducing slope to failure at about 0.6% strain. By comparison, the curve for the earlier unidirectional material [1] was linear to only about 0.2% strain and ultimate failure was at about 0.9% strain, but the shapes of the two curves are not dissimilar. The curve for the $(\pm 45,0_2)_s$ material shows features which resemble those obtained by many workers on CMC materials that exhibit significant amounts of cracking. The initial linear part of the curve extends to only 0.1% strain (similar to that for earlier $(0,90)_{3s}$ composites), and beyond this level there is an initial reduction in slope, followed first by a further slight increase and then by a subsequent gradual reduction in slope to failure at about 0.7% strain. For both composites, catastrophic failure occurs immediately on reaching the maximum stress. The scanning electron micrograph of the fracture surface of a sample of the $(\pm 45,0_2)_s$ composite given in Fig. 5 shows substantial amounts of fibre pull-out, but there is also evidence of much better fibre/matrix bonding than that illustrated for the earlier composites in our initial reports on SiC/borosilicate material. The complex mode of failure of this material is clearly seen in this photograph.

In Fig. 6 the transverse strains monitored by the 90° strain gauges mounted on the sample faces are plotted as functions of longitudinal strain for the two composites. The curves have been smoothed by Fourier-transform filtering to remove "judder" caused by the digital signal recording and processing. These curves

are quite different from those which we have obtained for the earlier Nicalon/borosilicate unidirectional and $(0,90)_{3s}$ composites, for unidirectional carbon fibre/borosilicate composites [1], and more recently for unidirectional and $(0,90)_{3s}$ laminates of SiC/CAS material [9]. For those materials, the transverse strain at first increased (in the negative sense, i.e. exhibiting normal Poisson contraction behaviour) but at some critical level the direction of the change was gradually reversed, the strain then beginning to increase in the positive sense, and in most cases the sample continued to expand beyond its original lateral dimension. This phenomenon we have ascribed [9] to the effect of a gradual relaxation of the residual thermal stresses built into the material during cooling from the final heat-treatment temperature (or, in the case of glass-matrix composites, cooling from the point at which all network motion is effectively frozen in. By contrast, the curves for these newer Nicalon/borosilicate materials show only negative dimensional changes as the samples are deformed to failure. Because the same fibre and matrix are involved in both kinds of transverse-strain behaviour, it is clear that models [12] ascribing the transverse-strain reversal to fibre "waviness" (variations in diameter along the length) and friction effects associated with it cannot be valid. The curve for the unidirectional material is substantially linear to failure (we ignore the slight instabilities in the upper curve in Fig. 6 which are probably due to experimental problems rather than genuine material behaviour), which implies a reasonably constant Poisson's ratio of about 0.2, as shown by Fig. 7. (The two curves in this figure have also been smoothed, as in the case of Fig. 6.)

3.2.4. Acoustic emission results

Curves of the total number of acoustic emission events as a function of strain are displayed on semilog plots in Fig. 8. The general form of the two curves is similar, and also resembles those presented in previous papers for the earlier unidirectional and $(0,90)_{3s}$ Nicalon/borosilicate composites [1], for unidirectional and 0/90 carbon/borosilicate composites [1], and also for SiC/CAS composites [9]. The important feature, as in the other cases, is that cracking events in these CMC composites begin to occur at very low strain levels, the threshold strain being about 0.02% for the curves in Fig. 8. There are minor differences between the curves for the two lay-ups, the overall level of AE activity being lower in the unidirectional material over the first half of the test, but the positions of the two curves are reversed at about 0.4% strain. The curve for the unidirectional material shows a pair of sudden jumps in level before a strain of about 0.2% is reached, but that for the $(\pm 45, 0_2)_s$ composite is smoother.

The AE event rates are plotted as a function of strain in Fig. 9. It can be seen here that while the two jumps in the cumulative AE curve for the unidirectional material referred to earlier are clearly associated with the two spikes on the event-rate curve, the major feature of this curve is, nevertheless, the single broad peak centred at about 0.4% strain. The spikes appear to represent minor instabilities. Much smaller spikes were also observed in the early stages of the event rate curve for the earlier unidirectional material [1], but in more recent tests on unidirectional

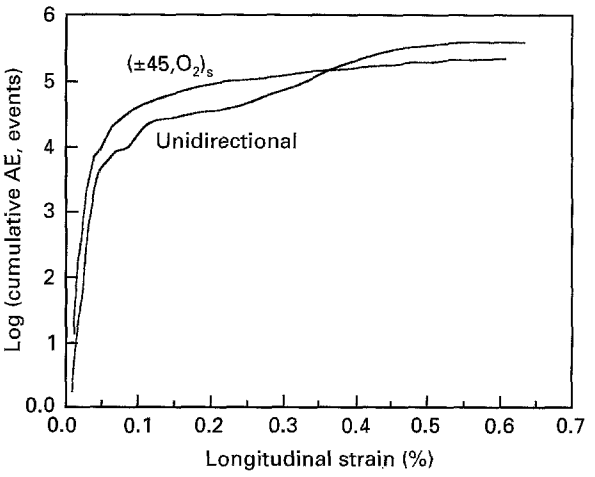

Figure 8 Cumulative acoustic emission count as a function of strain during tensile testing of unidirectional and $(\pm 45, 0_2)_s$ Nicalon/borosilicate composites.

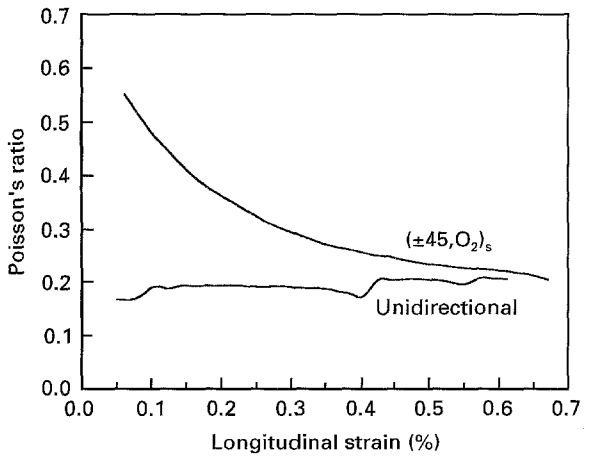

Figure 7 Apparent Poisson's ratio for unidirectional and $(\pm 45, 0_2)_s$ Nicalon/borosilicate composites as a function of axial strain.

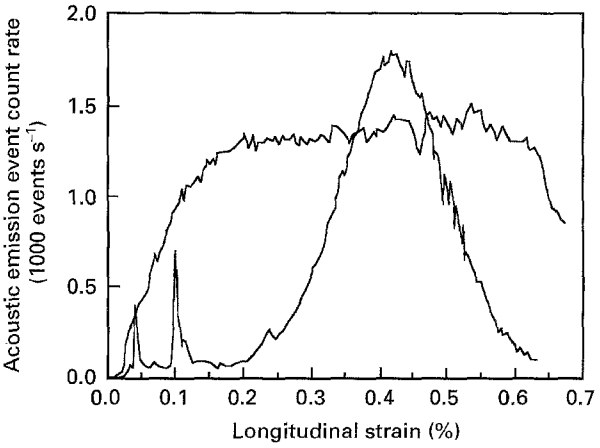

Figure 9 Acoustic emission event count rate as a function of tensile strain for unidirectional and $(\pm 45, 0_2)_s$ Nicalon/borosilicate composites.

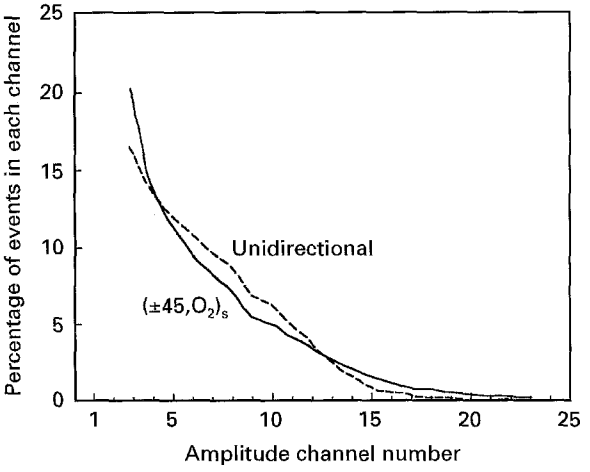

Figure 10 AE amplitude distribution (normalized) for tensile tests on unidirectional and $(\pm 45, 0_2)_s$ Nicalon/borosilicate composites.

SiC/CAS composites the only feature of the event rate curve is the single broad peak [9]. By contrast, the rate curve for the $(\pm 45, 0_2)_s$ composite rises rapidly, from very early in the test, and reaches a very broad plateau by about 0.2% strain. Beyond this the rate remains more or less constant at the high level of about 1200 events s^{-1} until just before failure.

The AE amplitude distribution diagrams associated with the tensile tests on the unidirectional and $(\pm 45, 0_2)_s$ composites are shown in Fig. 10. These are normalized to show the numbers of events in each of the 26 energy channels as percentages of the total numbers of events obtained for the test. The similarity of the distributions, which we have previously also observed for SiC/CAS materials, implies that the predominant mechanisms of deterioration under load are the same in both of these lay-ups.

4. Discussion

The desizing of Nicalon fibres prior to incorporation in a composite produces an oxygen-enriched layer at the surface of the fibre. Hot-pressing the fibre in the composite does not lead to a significant degradation in fibre strength, but there is a marked decrease in the Weibull shape factor (increase in variability) and this might be expected to reduce the composite strength. There may perhaps have been a more pronounced effect on strength during composite manufacture than is seen here if the HF etch used to extract the fibres had removed some of the surface defects introduced by manufacturing.

Cristobalite formation was found in all composite plates, and this was not surprising considering that hot-pressing experiments on plain borosilicate glass powder [4] suggest that 950 °C, the temperature at which the composite plates were produced [8], is actually the optimum pressing temperature for cristobalite formation. The presence of cristobalite leads to microcracking in the matrix, owing to the relief of stresses arising from the mismatch in thermal expansion coefficients between borosilicate glass ($3.2 \times 10^{-6}\ K^{-1}$) and cristobalite ($27 \times 10^{-6}\ K^{-1}$). Further cracks probably arise as a result of the large volume change associated with the $\alpha \rightarrow \beta$ cristobalite transformation at 277°C.

Three types of composite behaviour were identified in these studies. The first is that seen in R71(2), which has a low cristobalite content (about 10 vol %) and an intermediate interfacial friction stress value (about 8 MPa). The low cristobalite content means that few pre-existing microcracks are already present in the matrix, and once the failure-causing crack begins to propagate, it is unhindered by a pre-existing crack network. Once the crack impinges on a fibre, the interfacial bond is weak enough to deflect the crack, and consequently long, smooth fibre pull-outs are seen, with the matrix remaining intact.

The second type of failure is that seen for a composite with high cristobalite content (about 48 vol %) and a relatively high interfacial friction stress (about 12 MPa). In this composite there were many microcracks already present in the matrix which may have acted to initiate failure. When the propagating crack meets the fibre, the strong bond allows the crack to pass through the fibre with little recognition of the interface, breaking the fibre before it reaches its load-bearing capacity and producing a more brittle failure. Where pull-out did occur, adherent matrix particles were seen on fibre surfaces. Reference has already been made [2] to this kind of behaviour in an earlier paper on material described by Dawson *et al.* [7].

Composite R3(1) also had a cristobalite content of about 48 vol %, but a low interfacial friction stress (about 5 MPa). Again the matrix was highly microcracked, but in this case the propagating crack was deflected at the weak interface. Eventually a three-dimensional crack network is formed and the matrix becomes fragmented and falls away from the fibres, leaving long lengths of clean fibre to bear the load of failure. In this case high values of tensile and flexural strength are obtained, but these are meaningless, because the composite has lost structural integrity long before the failure load is reached.

The interfacial friction stress had been shown to play an important role in the fracture of the composite, high values leading to more brittle failures, lower values allowing pull-out. The differences in interfacial friction stress between the composites can be explained in terms of the chemical composition of the interface. The interface in a sample of a composite which had the highest value of interfacial friction stress also exhibited the lowest levels of carbon and sodium enrichment. Conversely, the interface of composite R3(1), with the lowest value of interfacial friction stress, had high levels of carbon and sodium, in addition to small traces of the matrix impurities calcium and potassium. Of the two elements, it is thought that carbon at the interface has a lubricating action, lowering the interfacial friction stress. The higher the carbon level, the lower the stress. Carbon is formed by the reaction

$$SiC(s) + O_2(g) \rightarrow SiO_2(s) + C(s) \quad (1)$$

as observed by Cooper and Chyung [13] in other Nicalon-reinforced systems. Sodium enrichment occurs as a result of diffusion of mobile sodium ions from

the matrix to leave a soidum-denuded region adjacent to the fibre.

In our earlier discussions of transverse-strain behaviour we have expressed anxiety about the peculiar variations of ν_{12} with strain and reservations as to the significance of measured values of ν_{12} as a design parameter, but it is clear that in the case of these later unidirectional Nicalon/borosilicate materials this would not be an issue. The transverse strain for the $(\pm 45,0_2)_s$ composite also varies only in a negative sense with axial strain, all the way to failure, but in this case the curve is not linear over the initial 0.2% or so of axial strain and shows signs of flattening out just prior to failure. In this case, therefore, it appears that the material is exhibiting some of the features that we have remarked on before, but fails before reversal of the transverse strain can occur.

5. Conclusions

1. The interfacial bonding in recent examples of a Nicalon fibre-reinforced borosilicate glass composite is substantially better than that of earlier materials processed by the same manufacturer. This is demonstrated by the vastly improved level of shear stiffness (by a factor of 2–3) and the higher level of interlaminar shear strength (some 50%–100% improvement). There is, however, an accompanying deterioration in tensile and flexural strength.

2. It is clear that the fracture mode of these Nicalon/borosilicate composites is strongly influenced by cristobalite content and the properties of the interface, both of which are controlled to a large extent by the manufacturing parameters.

3. In common with the earlier composites, acoustic emission monitoring indicates that matrix cracking commences at very low strain levels during deformation. It is now clear, however, that this is inherent in the material, and is not a consequence of the presence of high levels of cristobalite.

4. The transverse-strain behaviour of the newer Nicalon/borosilicate appears to be different from that of both the earlier material and SiC/CAS composites in that ε_{22} increases linearly (in a negative sense) to the point of failure of the composite, without showing the familiar reversal and expansion behaviour previously discussed.

Acknowledgement

The authors are grateful to Rolls Royce plc for their financial support of this work, for the provision of Nicalon/borosilicate-glass composites, and for permission to publish this paper.

References

1. F. A. HABIB, R. G. COOKE and B. HARRIS, *Br. Ceram. Trans. J.* **89** (1990) 115.
2. S. M. BLEAY and V. D. SCOTT, *J. Mater. Sci* **26** (1991) 2229.
3. *Idem., ibid.* **26** (1991) 3544.
4. S. G. CLARKE, S. M. BLEAY and V. D. SCOTT, *J. Mater. Sci. Lett.* **10** (1991) 149.
5. T. KISHI, N. TAKEDA and Y. KAGAWA, (eds), Proceedings of NEDO Japan/USA Joint Research Symposium (1993), Proceedings of the Third Japan International SAMPE Symposium, "Advanced Materials — New Processes and Reliability", Vol. 1 (Japan Chapter of SAMPE, Tokyo).
6. R. A. J. SAMBELL, A. BRIGGS, D. C. PHILLIPS and D. H. BOWEN, *J. Mater. Sci.* **7** (1972) 676.
7. D. M. DAWSON, R. F. PRESTON and A. PURSER, *Ceram. Eng. Sci. Proc.* **8** (1987) 815.
8. B. A. FORD, R. G. COOKE and S. NEWSAM, *Brit. Ceram. Proc.* **39** (1987) 229.
9. B. HARRIS, F. A. HABIB and R. G. COOKE, *Proc. R. Soc. (Lond.)* **A437** (1992) 109.
10. "Standard Test Method for Tensile Strength And Young's Modulus For High Modulus Single Filament Materials", ASTM D3379-75 (American Society for Testing and Materials, New York, 1981).
11. D. B. MARSHALL and A. G. EVANS, *J. Am. Ceram. Soc.* **68** (1985) 225.
12. B. F. SORENSEN, *Scripta Metall. Mater.* **28** (1993) 435.
13. R. F. COOPER and K. CHYUNG, *J. Mater. Sci.* **22** (1987) 3148.

Received 9 January
and accepted 18 March 1996